

The 3-State Square-Lattice Potts Antiferromagnet at Zero Temperature

Jesús Salas

Departamento de Física de la Materia Condensada and

Departamento de Física Teórica

Facultad de Ciencias

Universidad de Zaragoza

50009 Zaragoza SPAIN

JESUS@JUPITER.UNIZAR.ES

Alan D. Sokal

Department of Physics

New York University

4 Washington Place

New York, NY 10003 USA

SOKAL@NYU.EDU

February 1, 2008

Abstract

We study the 3-state square-lattice Potts antiferromagnet at zero temperature by a Monte Carlo simulation using the Wang-Swendsen-Kotecký cluster algorithm, on lattices up to 1024×1024 . We confirm the critical exponents predicted by Burton and Henley based on the height representation of this model.

Key Words: Antiferromagnetic Potts model, critical ground state, height representation, critical exponent, Monte Carlo, Wang-Swendsen-Kotecký algorithm, cluster algorithm.

1 Introduction

Antiferromagnetic Potts models [1, 2, 3] are much less well understood than their ferromagnetic counterparts. One reason for this is that the behavior depends strongly on the microscopic lattice structure, in contrast to the universality typically enjoyed by ferromagnets. As a result, many basic questions have to be investigated case-by-case: Is there a phase transition at finite temperature, and if so, of what order? What is the nature of the low-temperature phase? If there is a critical point, what are the critical exponents and the universality classes? Can these exponents be understood (for two-dimensional models) in terms of conformal field theory?

One thing is known rigorously [4, 5]: for q large enough (how large depends on the lattice in question), the antiferromagnetic q -state Potts model has a unique infinite-volume Gibbs measure and exponential decay of correlations at all temperatures, *including zero temperature*: the system is disordered as a result of the large ground-state entropy.¹ However, for smaller values of q , phase transitions can and do occur. One expects that for each lattice \mathcal{L} there will be a value $q_c(\mathcal{L})$ such that

- (a) For $q > q_c(\mathcal{L})$ the model has exponential decay of correlations uniformly at all temperatures, including zero temperature.
- (b) For $q = q_c(\mathcal{L})$ the model has a critical point at zero temperature.
- (c) For $q < q_c(\mathcal{L})$ any behavior is possible. Often (though not always) the model has a phase transition at nonzero temperature, which may be of either first or second order.

The problem, for each lattice, is to find $q_c(\mathcal{L})$ and to determine the precise behavior for each $q \leq q_c(\mathcal{L})$.

For the common two-dimensional lattices, strong theoretical arguments² — which, however, fall short of a rigorous proof — yield the following predictions for $q_c(\mathcal{L})$:

$$q_c(\mathcal{L}) = \begin{cases} (3 + \sqrt{5})/2 \approx 2.618\dots & \text{for the hexagonal lattice} \\ 3 & \text{for the square lattice} \\ 3 & \text{for the Kagomé lattice} \\ 4 & \text{for the triangular lattice} \end{cases} \quad (1.1)$$

Monte Carlo simulations have confirmed numerically that the 3-state square-lattice model has a zero-temperature critical point [6, 7], and that the 4-state square-lattice model [6, 7] and the 3-state hexagonal-lattice model [8, 9] are non-critical uniformly down to zero temperature.³

¹ This behavior has been proven for $q \geq 4$ on the hexagonal lattice, $q \geq 6$ on the Kagomé lattice, $q \geq 7$ on the square lattice, and $q \geq 11$ on the triangular lattice [5]. However, these bounds are presumably *not* sharp: see equation (1.1) below.

² Summarized in the introduction to [5].

³ The Monte Carlo simulations of the 3-state hexagonal-lattice model reported in Ref. [8] give no evidence of any *first-order* phase transition as the temperature is varied from infinity to zero;

Two-dimensional models with zero-temperature critical points are of particular interest, as they can in most cases be mapped onto a “height” (or “interface” or “SOS-type”) model [10, 11, 12, 13, 14, 15, 16, 17, 18, 19, 20, 21, 22, 23, 24, 25, 26, 27]. If this height model lies in its “rough” phase — a question that has to be investigated on a case-by-case basis — then its long-distance behavior is that of a massless Gaussian with some (*a priori* unknown) “stiffness” $K > 0$. The critical operators can then be identified via the height mapping, and the corresponding critical exponents can be predicted in terms of the single parameter K . In particular, if we know (by some other means) one of these exponents, then we can deduce the rest.

Height representations thus give a means for recovering a sort of universality for some (but not all) antiferromagnetic Potts models and for understanding their critical behavior in terms of conformal field theory. All the nonuniversal details of the microscopic lattice structure are encoded in the height representation and in the stiffness parameter K . Given these, everything can be understood in terms of the universal behavior of massless Gaussian fields.

The plan of this paper is as follows: In Section 2 we present briefly the general theory of height representations and then work out in detail the case of the 3-state square-lattice Potts antiferromagnet. Our presentation is based on the work of Henley and collaborators [19, 20, 23, 24, 26, 27], supplemented by a few minor innovations of our own. In the remainder of the paper, our goal is to test, by Monte Carlo simulation, the critical exponents predicted by Burton and Henley [26] for the three relevant operators in the 3-state square-lattice Potts antiferromagnet at zero temperature. In Section 3 we describe our simulations, and in Section 4 we analyze the data.

2 Height Representations

Many two-dimensional models with zero-temperature critical points can be mapped onto a “height” model: these include the triangular-lattice Ising antiferromagnet [11, 12], the triangular-lattice spin- S Ising antiferromagnet [24], the 3-state square-lattice Potts antiferromagnet [10, 13, 26], the 3-state Kagomé-lattice Potts antiferromagnet [16, 20], the 4-state triangular-lattice Potts antiferromagnet [27], the 4-state Potts antiferromagnet on the covering lattice of the square lattice [19, 20], a constrained 4-state Potts antiferromagnet on the square lattice [26], a special 6-vertex model [20], and various dimer models [14, 15, 23, 25] and fully packed loop models [17, 18, 21, 22]. Here we shall explain briefly the basic principles underlying the construction of such mappings and their use to extract critical exponents. We shall then work out in detail the case of the 3-state square-lattice Potts antiferromagnet.

this behavior is consistent with the theoretical prediction that the model has exponential decay of correlations uniformly down to zero temperature. However, these authors did not measure the correlation length or the staggered susceptibility, so no direct test of the non-criticality at zero temperature was made. Such a direct test is being made in Ref. [9].

2.1 General Theory

The first step is to define a map assigning to each zero-temperature spin configuration $\{\sigma(x)\}$ a corresponding microscopic height configuration $\{h(x)\}$. This *height rule* is usually defined by local increments, i.e. one prescribes the change $\Delta h \equiv h(y) - h(x)$ in going from a site x to a neighboring site y in terms of the spin variables $\sigma(x)$ and $\sigma(y)$. For such a rule to be well-defined, one must verify that in all cases the net increment Δh around any closed loop is zero.⁴ The height variables $h(x)$ lie in some discrete set $\mathcal{H} \subset \mathbf{R}^D$ (for some suitable dimension D), which we call the *height lattice*.

The next step is to identify the so-called *ideal states*: these are ground-state configurations (or families of configurations) of the original spin model whose corresponding height configurations are macroscopically “flat” (i.e. have zero net slope) and which maximize the entropy density (in the sense of maximizing the number of ground states that can be obtained from the ideal states by local modifications of the spins). We label each ideal state by its average height $h \in \mathbf{R}^D$, and we define the *ideal-state lattice* $\mathcal{I} \subset \mathbf{R}^D$ to be the set of all average heights of ideal states. The *equivalence lattice*

$$\mathcal{E} = \{a \in \mathbf{R}^D : a + \mathcal{I} = \mathcal{I}\} \quad (2.1)$$

is the subgroup of \mathbf{R}^D summarizing the underlying periodicity of \mathcal{I} .

We now guess that, in typical configurations of the spin model, the lattice is subdivided into reasonably large domains in which the spin configuration closely resembles one of the ideal states. It follows that typical configurations of the height model are given by domains in which the height $h(x)$ exhibits small fluctuations around one of the values in the ideal-state lattice. We therefore expect that a suitably defined coarse-grained height variable $\bar{h}(x)$ will take values in or near the ideal-state lattice \mathcal{I} , except at boundaries between domains. The long-wavelength behavior of the height model is thus postulated to be controlled by an effective coarse-grained Hamiltonian of the form

$$H = \int d^2x \left[\frac{K}{2} \sum_{i=1}^D |\nabla \bar{h}_i|^2 + V_{\text{lock}}(\bar{h}(x)) \right], \quad (2.2)$$

where we have made explicit the components of the macroscopic height $\bar{h} = (\bar{h}_1, \bar{h}_2, \dots, \bar{h}_D)$. The gradient term in (2.2) takes into account the entropy of small fluctuations around the ideal states; the second term is the so-called *locking potential*, which favors the heights to take their values in \mathcal{I} . We then expect that there exists some constant K_r such that for $K < K_r$ (resp. $K > K_r$) the locking potential is irrelevant (resp. relevant) in the renormalization-group sense. Thus, if $K < K_r$ our surface model is “rough” and its long-wavelength behavior can be described by a massless Gaussian model [28, 20] with D components:

$$\langle [\bar{h}_i(x) - \bar{h}_i(y)] [\bar{h}_j(x) - \bar{h}_j(y)] \rangle \approx \frac{\delta_{ij}}{\pi K} \log |x - y| \quad (2.3)$$

⁴ In fact, this property usually holds for free boundary conditions but *not* for periodic boundary conditions. We shall hereafter neglect this latter subtlety, by imagining that we are working always in infinite volume.

for $|x - y| \gg 1$; in this case, the original zero-temperature spin system is critical. If, on the other hand, $K > K_r$, then the surface model is in its “smooth” phase, exhibiting long-range order

$$\langle \bar{h}(x) \rangle = \mathbf{h}_0 \quad (2.4)$$

and *bounded* fluctuations around this ordered state:

$$\langle [\bar{h}(x) - \bar{h}(y)]^2 \rangle \text{ bounded as } |x - y| \rightarrow \infty ; \quad (2.5)$$

correspondingly, the spin system is “locked” into small fluctuations around one of the ideal states. At $K = K_r$ the surface model undergoes a roughening transition.⁵

Let us note, finally, that a given ideal state can be represented by many different average heights $h \in \mathcal{I}$. More precisely, suppose that in some domain we have a particular ideal state X and that its average height is $h_0 \in \mathcal{I}$. Now let us pass through various other domains of the lattice, coming back finally to a domain in which the ideal state is again X . We will find the average height in this latter domain to lie in the set $h_0 + \mathcal{R}$, where \mathcal{R} is a particular subgroup of \mathcal{E} that we call the *repeat lattice*; we will also find, conversely, that whenever we enter a domain in which the average height lies in $h_0 + \mathcal{R}$, that domain is in ideal state X . It follows that the ideal states are in one-to-one correspondence with the cosets \mathcal{I}/\mathcal{R} .

The coarse-grained correlation functions of local operators in the spin language can be understood in terms of the correlation functions of local operators of the coarse-grained heights. The important point is that these latter operators should have the periodicity of the repeat lattice \mathcal{R} . This means that the Fourier expansion of such an operator \mathbf{O} ,

$$\mathbf{O}(x) = \sum_{G \in \mathcal{R}^\circ} O_G e^{iG \cdot \bar{h}(x)} , \quad (2.6)$$

contains only wavevectors belonging to the reciprocal lattice of the repeat lattice,

$$\mathcal{R}^\circ \equiv \{G \in \mathbf{R}^D : G \cdot a \in 2\pi\mathbf{Z} \text{ for all } a \in \mathcal{R}\} . \quad (2.7)$$

On the other hand, two wavevectors whose difference belongs to the reciprocal lattice of the equivalence lattice,

$$\mathcal{E}^\circ \equiv \{G \in \mathbf{R}^D : G \cdot a \in 2\pi\mathbf{Z} \text{ for all } a \in \mathcal{E}\} , \quad (2.8)$$

give rise to vertex operators $\exp[iG \cdot \bar{h}(x)]$ having identical long-distance behavior. The vertex operators of the height model are thus in one-to-one correspondence with the cosets $\mathcal{R}^\circ/\mathcal{E}^\circ \simeq (\mathcal{E}/\mathcal{R})^\circ$.

Now, provided that the height model is in the rough phase ($K < K_r$), the correlation functions of the vertex operators $\exp[iG \cdot \bar{h}(x)]$ are given by

$$\langle e^{iG \cdot \bar{h}(0)} e^{-iG' \cdot \bar{h}(x)} \rangle = \delta_{G,G'} \exp \left[-\frac{G^2}{2} \langle [\bar{h}(0) - \bar{h}(x)]^2 \rangle \right] \sim \delta_{G,G'} |x|^{-G^2/(2\pi K)} . \quad (2.9)$$

⁵ Note that the only alternatives for the spin model are criticality and long-range order. Thus, if there exists a height representation, the original spin model cannot be disordered at zero temperature.

It follows that the critical behavior of the operator \mathbf{O} will be given by the most relevant vertex operator $\exp[iG \cdot \bar{h}(x)]$ appearing in its Fourier expansion with a nonzero coefficient:

$$\langle \mathbf{O}(0) \mathbf{O}(x)^* \rangle \sim |x|^{-\eta_{\mathbf{O}}} \quad (2.10)$$

where

$$\eta_{\mathbf{O}} = \min_{O_G \neq 0} \frac{G^2}{2\pi K} . \quad (2.11)$$

(The scaling dimension is $x_{\mathbf{O}} = \eta_{\mathbf{O}}/2$, and the operator is relevant in case the renormalization-group eigenvalue $d - x_{\mathbf{O}} = 2 - x_{\mathbf{O}}$ is > 0 .) This formula implies that we can write *all* the critical exponents in terms of a single parameter K . If one exponent is known, then all of them are.

In particular, the locking potential V_{lock} has the periodicity of the ideal-state lattice \mathcal{I} ; its Fourier expansion (2.6) has contributions only from wavevectors G belonging to \mathcal{E}° . Let $a_{\mathcal{E}^\circ}$ be the length of the smallest nonzero vector in \mathcal{E}° . Now, the roughening transition occurs exactly where the locking potential is marginal, i.e. where $\eta_{V_{\text{lock}}} = 4$. It follows that

$$K_r = \frac{a_{\mathcal{E}^\circ}^2}{8\pi} . \quad (2.12)$$

If $K < K_r$, the locking potential is irrelevant, with scaling dimension

$$x_{V_{\text{lock}}} = 2K_r/K > 2 . \quad (2.13)$$

It induces corrections to scaling $\sim L^{2-x_{V_{\text{lock}}}}$, where L is a suitable length scale.

In addition to vertex operators $\exp[iG \cdot \bar{h}(x)]$, there is another type of local operator that makes sense in the massless Gaussian model: powers of gradients of \bar{h} .⁶ In particular, the operator $(\nabla \bar{h})^{2n}$ has scaling dimension

$$x_{(\nabla \bar{h})^{2n}} = 2n \quad (2.14)$$

and hence $\eta_{(\nabla \bar{h})^{2n}} = 4n$. It follows that all these operators are irrelevant, except the operator $(\nabla \bar{h})^2$, which is marginal. Since these operators respect the lattice symmetries, they can appear in the effective Hamiltonian and thereby induce corrections to scaling. The leading such operator is $(\nabla \bar{h})^4$, with scaling dimension $x_{(\nabla \bar{h})^4} = 4$; it induces corrections $\sim L^{2-x_{(\nabla \bar{h})^4}} = L^{-2}$.

Assuming that we have not overlooked any irrelevant operators that could appear in the effective Hamiltonian, we conclude that the leading corrections to scaling behave as $L^{-\Delta}$, with

$$\Delta = \min(x_{V_{\text{lock}}} - 2, x_{(\nabla \bar{h})^4} - 2) = \min\left(\frac{2K_r}{K} - 2, 2\right) . \quad (2.15)$$

We remark, finally, the height representation can also be applied to these models at *nonzero* temperature. In that case one must consider also the fugacity of *defects*: that is, of places where the zero-temperature constraints are violated [20, 27]. Very often the defect fugacity is a *relevant* operator.

⁶ The height \bar{h} itself is ill-defined as a field in dimension $d \leq 2$, due to infrared divergences. But gradients $\nabla \bar{h}, \nabla \nabla \bar{h}, \dots$ are well-defined.

2.2 Three-State Square-Lattice Potts Antiferromagnet

The height representation of the 3-state square-lattice Potts antiferromagnet at zero temperature is very simple [10, 26]. Let the Potts spins $\sigma(x)$ take values in the set $\{0, 1, 2\}$. The microscopic height variables $h(x)$ are then assigned as follows: At the origin we take $h(0) = 0, 4, 2 \pmod{6}$ according as $\sigma(0) = 0, 1, 2$; this ensures that

$$h(0) = \sigma(0) \pmod{3} \quad (2.16a)$$

$$h(0) = 0 \pmod{2} \quad (2.16b)$$

We then define the increment in height in going from a site x to a nearest neighbor y by

$$h(x) - h(y) = \sigma(x) - \sigma(y) \pmod{3} \quad (2.17a)$$

$$h(x) - h(y) = \pm 1 \quad (2.17b)$$

This is well-defined (in free boundary conditions) because the change Δh around any plaquette is zero.⁷ It follows from (2.16) and (2.17) that

$$h(x) = \sigma(x) \pmod{3} \quad (2.18a)$$

$$h(x) = x_1 + x_2 \pmod{2} \quad (2.18b)$$

for any site $x = (x_1, x_2)$. In particular, the height $h(x)$ is uniquely determined mod 6 once we know the spin value $\sigma(x)$ and the parity of x , and conversely. The height lattice \mathcal{H} is clearly equal to \mathbf{Z} .

There are six ideal states, given by 0/12 (spins on the even sublattice all equal to 0, spins on the odd sublattice chosen randomly between 1 and 2) and its permutations.⁸ In an ideal state, the height is constant on the ordered sublattice and fluctuates randomly ± 1 around this level on the disordered sublattice. The average height of an ideal state is thus equal to its height on the ordered sublattice; it then follows from (2.18) that there is a one-to-one correspondence between ideal states and average heights mod 6 (see Figure 1).⁹ The ideal-state lattice \mathcal{I} is thus also \mathbf{Z} , as is the equivalence lattice \mathcal{E} , while the repeat lattice \mathcal{R} is $6\mathbf{Z}$. The corresponding reciprocal lattices are $\mathcal{E}^\circ = 2\pi\mathbf{Z}$ and $\mathcal{R}^\circ = (\pi/3)\mathbf{Z}$.

There are three relevant operators (in the renormalization-group sense) appearing in this model (see Table 1) [10, 26]:

$$\mathbf{M}_{stagg}(x) = (-1)^{x_1+x_2} \vec{\sigma}(x) \quad (2.19)$$

$$\mathbf{M}_u(x) = \vec{\sigma}(x) \quad (2.20)$$

$$\mathbf{P}_{stagg}(x) = \frac{1}{4}(-1)^{x_1+x_2} \sum_{y \text{ nnn of } x} (2\delta_{\sigma(x), \sigma(y)} - 1) \quad (2.21)$$

⁷ If four numbers ± 1 add up to 0 mod 3, they must necessarily be two +1's and two -1's, hence add up to 0.

⁸ States like 0/1 are not ideal states because they do not have maximal entropy density.

⁹ This fact was proven, in a different way, by Burton and Henley [26, Appendix B.2].

where we have represented the Potts spin at site $x = (x_1, x_2)$ by a unit vector in the plane

$$\vec{\sigma}(x) = \left(\cos \frac{2\pi}{3} \sigma(x), \sin \frac{2\pi}{3} \sigma(x) \right). \quad (2.22)$$

The first operator is the staggered magnetization; the staggering corresponds to a momentum $\mathbf{k}_{stagg} = (\pi, \pi)$. The second operator is the uniform magnetization. The third operator is a staggered sum over diagonal next-nearest-neighbor correlations (i.e. over y with $|y - x| = \sqrt{2}$); we call it the staggered polarization. In an ideal state, it takes the average value +1 (resp. -1) according as it is the even (resp. odd) sublattice that is ordered.¹⁰

We can relate these observables directly to the *microscopic* height variables $h(x)$ by exact identities. For the vertex operators with $G = \pm\pi/3, \pm 2\pi/3, \pm\pi$ we have

$$e^{\pm i(\pi/3)h(x)} = M_{stagg}^{(1)}(x) \mp iM_{stagg}^{(2)}(x) \quad (2.23)$$

$$e^{\pm i(2\pi/3)h(x)} = M_u^{(1)}(x) \pm iM_u^{(2)}(x) \quad (2.24)$$

$$e^{\pm i\pi h(x)} = (-1)^{x_1+x_2} \quad (2.25)$$

Here (2.24) and (2.25) follow immediately from (2.18a) and (2.18b), respectively, while (2.23) follows by multiplying these two and taking the complex conjugate. Of course, the strictly local operator (2.25) is trivial, but we can define a nontrivial almost-local operator with the same ($G = \pi$) long-distance behavior:

$$e^{\pm i(\pi/2)[h(x)+h(y)]} = (-1)^{x_1+x_2} (2\delta_{\sigma(x),\sigma(y)} - 1) \quad (2.26)$$

for diagonal next-nearest-neighbor sites x, y .¹¹ It follows that $G = \pi$ corresponds to the staggered polarization.

Remark. It is also of interest to define almost-local operators living on plaquettes. Let x be a lattice site, and let $\square(x) \equiv \{(x_1, x_2), (x_1+1, x_2), (x_1+1, x_2+1), (x_1, x_2+1)\}$ be the plaquette whose lower-left corner is x . We then define the average height $\tilde{h}(x)$ over that plaquette as

$$\tilde{h}(x) \equiv \frac{1}{4} \sum_{y \in \square(x)} h(y). \quad (2.27)$$

It is easy to see that $\tilde{h}(x)$ takes values in $\mathbf{Z} \cup (\mathbf{Z} + \frac{1}{2})$: namely, it takes an integer (resp. half-integer) value if there are three (resp. two) distinct spin values $\sigma(y)$ on the

¹⁰ Burton and Henley [26] chose a slightly different definition of this operator: $\mathbf{P}_{stagg}(x) = (1/4)(-1)^{x_1+x_2} \sum_{y \text{ nnn of } x} \delta_{\sigma(x),\sigma(y)}$.

¹¹ PROOF: Next-nearest-neighbor sites x, y always satisfy $h(y) - h(x) = 0$ or ± 2 : the former case occurs when $\sigma(x) = \sigma(y)$, and the latter when $\sigma(x) \neq \sigma(y)$. It follows that

$$e^{\pm i(\pi/2)[h(y)-h(x)]} = 2\delta_{\sigma(x),\sigma(y)} - 1.$$

Now multiply this by (2.25).

plaquette $\square(x)$. Indeed, the value of $\tilde{h}(x)$ is uniquely determined mod 6 by the spin content of the plaquette: see Figure 2. Finally, for two adjacent plaquettes $\square(x)$ and $\square(x')$, we have

$$\Delta\tilde{h} \equiv \tilde{h}(x') - \tilde{h}(x) = \begin{cases} 0, \pm\frac{1}{2}, \pm 1 & \text{if } \tilde{h}(x) \in \mathbf{Z} \\ 0, \pm\frac{1}{2} & \text{if } \tilde{h}(x) \in \mathbf{Z} + \frac{1}{2} \end{cases} \quad (2.28)$$

The upshot of this construction is that, because $\tilde{h}(x)$ takes half-integral as well as integral values, vertex operators $\exp[iG\tilde{h}(x)]$ and $\exp[iG'\tilde{h}(x)]$ are equivalent only if $G = G' \bmod 4\pi$, rather than $\bmod 2\pi$ as before; so we can define operators up to $|G| = 2\pi$ rather than only $|G| = \pi$. (However, as will be seen below, all these “extra” operators are irrelevant.) We have

$$e^{\pm i(\pi/3)\tilde{h}(x)} = \frac{\sum_{y \in \square(x)} M_{stagg}^{(1)}(y) \mp iM_{stagg}^{(2)}(y)}{\left| \sum_{y \in \square(x)} M_{stagg}^{(1)}(y) \mp iM_{stagg}^{(2)}(y) \right|} = \frac{\sum_{y \in \square(x)} M_{stagg}^{(1)}(y) \mp iM_{stagg}^{(2)}(y)}{3 + (2\sqrt{3} - 3)\delta_{\sigma(x),\sigma(x'')}\delta_{\sigma(x'),\sigma(x''')}} \quad (2.29)$$

$$e^{\pm i(2\pi/3)\tilde{h}(x)} = \frac{\sum_{y \in \square(x)} M_u^{(1)}(y) \pm iM_u^{(2)}(y)}{\left| \sum_{y \in \square(x)} M_u^{(1)}(y) \pm iM_u^{(2)}(y) \right|} = \frac{\sum_{y \in \square(x)} M_u^{(1)}(y) \pm iM_u^{(2)}(y)}{1 + \delta_{\sigma(x),\sigma(x'')}\delta_{\sigma(x'),\sigma(x''')}} \quad (2.30)$$

$$e^{\pm i\pi\tilde{h}(x)} = (-1)^{x_1+x_2} [\delta_{\sigma(x),\sigma(x'')} - \delta_{\sigma(x'),\sigma(x''')} \pm i\delta_{\sigma(x),\sigma(x'')}\delta_{\sigma(x'),\sigma(x''')}\Delta(\sigma(x') - \sigma(x))] \quad (2.31)$$

$$e^{\pm i(4\pi/3)\tilde{h}(x)} = e^{\pm i(2\pi)\tilde{h}(x)} e^{\mp i(2\pi/3)\tilde{h}(x)} = \frac{\sum_{y \in \square(x)} M_u^{(1)}(y) \mp iM_u^{(2)}(y)}{1 - 3\delta_{\sigma(x),\sigma(x'')}\delta_{\sigma(x'),\sigma(x''')}} \quad (2.32)$$

$$e^{\pm i(5\pi/3)\tilde{h}(x)} = e^{\pm i(2\pi)\tilde{h}(x)} e^{\mp i(2\pi/3)\tilde{h}(x)} = \frac{\sum_{y \in \square(x)} M_{stagg}^{(1)}(y) \pm iM_{stagg}^{(2)}(y)}{3 - (2\sqrt{3} + 3)\delta_{\sigma(x),\sigma(x'')}\delta_{\sigma(x'),\sigma(x''')}} \quad (2.33)$$

$$e^{\pm i(2\pi)\tilde{h}(x)} = 1 - 2\delta_{\sigma(x),\sigma(x'')}\delta_{\sigma(x'),\sigma(x''')} \quad (2.34)$$

where we have labelled the sites around the plaquette $\square(x)$ as x, x', x'', x''' in cyclic order, and in (2.31) we have used the shorthand $\Delta(n) = \pm 1$ according as $n = \pm 1 \bmod 3$.

We can now read off the predictions for critical exponents. The staggered magnetization corresponds to $G = \pi/3 = a_{\mathcal{R}^\circ}$ (this is the smallest nonzero vector in \mathcal{R}°), hence $\eta_{\mathbf{M}_{stagg}} = \pi/(18K)$. On the other hand, den Nijs *et al.* [10] and Park and Widom [29] obtained the exact value $\eta_{\mathbf{M}_{stagg}} = 1/3$ by means of a mapping to the 6-vertex

model. It follows that the height model corresponding to the 3-state square-lattice Potts antiferromagnet at zero temperature has stiffness $K = \pi/6$. (In particular, we have $K < K_r = \pi/2$, so the height model lies in its rough phase.) By the usual scaling law we obtain the susceptibility exponent $(\gamma/\nu)_{\text{stagg}} = 2 - \eta_{\mathbf{M}_{\text{stagg}}} = 5/3$. This value has been numerically verified by several authors [30, 31, 6, 7].

The uniform magnetization corresponds to $G = 2\pi/3 = 2a_{\mathcal{R}^\circ}$. (In this model the ideal states have a nonzero net magnetization, which, however, is the same for A/BC and BC/A; the uniform magnetization is thus periodic on the ideal-state lattice with period 3.) It follows that $\eta_{\mathbf{M}_u} = 4\eta_{\mathbf{M}_{\text{stagg}}} = 4/3$ and $(\gamma/\nu)_u = 2 - \eta_{\mathbf{M}_u} = 2/3$ [10]. It is interesting that the *uniform* magnetization is predicted to have a divergent susceptibility in this *antiferromagnetic* model. We are not aware of any numerical test of this prediction in the literature.

The staggered polarization corresponds to $G = \pi = 3a_{\mathcal{R}^\circ}$. We have $\eta_{\mathbf{P}_{\text{stagg}}} = 9\eta_{\mathbf{M}_{\text{stagg}}} = 3$ and hence $(\gamma/\nu)_{\mathbf{P}_{\text{stagg}}} = 2 - \eta_{\mathbf{P}_{\text{stagg}}} = -1$ [26]. This means that the “susceptibility” for this operator does not diverge, but tends to a finite value with a power-law correction $\sim L^{-1}$ (where L is the linear lattice size). This prediction has not, to our knowledge, been checked numerically in the literature.

These are the *only* relevant vertex operators in the model. Indeed, a vertex operator $\exp[iG \cdot \bar{h}(x)]$ is relevant if and only if $\eta = G^2/(2\pi K) < 4$; or, writing $G = na_{\mathcal{R}^\circ}$ with n integer, we need $|n| < \sqrt{8\pi K}/a_{\mathcal{R}^\circ}$. The values $K = \pi/6$ and $a_{\mathcal{R}^\circ} = \pi/3$ then imply that we must have $|G| < 2\pi/\sqrt{3}$, or $|n| < \sqrt{12}$.

The equivalence lattice has lattice spacing $a_{\mathcal{E}} = 1$, so that the wavevector corresponding to the locking potential is $G = 2\pi = 6a_{\mathcal{R}^\circ}$ and hence $\eta_{V_{\text{lock}}} = 36\eta_{\mathbf{M}_{\text{stagg}}} = 12 > 4$. So, V_{lock} is a (strongly) irrelevant operator.

Remark. The foregoing predictions contain, at first glance, a serious paradox. The correlation functions of the *microscopic* staggered and uniform magnetizations,

$$G_{\text{stagg}}(x) = \langle \mathbf{M}_{\text{stagg}}(0) \cdot \mathbf{M}_{\text{stagg}}(x) \rangle \quad (2.35)$$

$$G_u(x) = \langle \mathbf{M}_u(0) \cdot \mathbf{M}_u(x) \rangle \quad (2.36)$$

obviously satisfy

$$G_{\text{stagg}}(x) = (-1)^{x_1+x_2} G_u(x). \quad (2.37)$$

How, then, can $G_{\text{stagg}}(x)$ decay at large $|x|$ like $|x|^{-1/3}$ while $G_u(x)$ decays like $|x|^{-4/3}$? The answer, presumably, is that the correlation functions contain *both* terms [10]:

$$G_{\text{stagg}}(x) \sim |x|^{-1/3} + (-1)^{x_1+x_2} |x|^{-4/3} + \dots \quad (2.38)$$

$$G_u(x) \sim (-1)^{x_1+x_2} |x|^{-1/3} + |x|^{-4/3} + \dots \quad (2.39)$$

It is only when one passes to *coarse-grained* correlation functions, by smearing over several nearby lattice sites, that the oscillatory terms are replaced by much-more-rapidly decaying remnants, leaving¹²

$$\bar{G}_{\text{stagg}}(x) \sim |x|^{-1/3} + |x|^{-10/3} + \dots \quad (2.40)$$

¹² In order to get the maximum additional decay (namely, two powers of $|x|$), it is necessary to smear over an $m \times n$ block with m and n both *even*.

$$\bar{G}_u(x) \sim |x|^{-7/3} + |x|^{-4/3} + \dots \quad (2.41)$$

A similar cancellation of oscillatory terms occurs, of course, when one looks at the susceptibilities.

3 Numerical Simulations

In order to test all these predictions, we have carried out a Monte Carlo simulation of the 3-state square-lattice Potts antiferromagnet at zero temperature, on periodic $L \times L$ lattices with L ranging from 4 to 1024. We made our simulation using the Wang-Swendsen-Kotecký (WSK) cluster algorithm [30, 31], which is ergodic at $T = 0$ on any bipartite graph, and in particular on a periodic square lattice whenever the linear lattice size L is *even* [26, 7].¹³

For each lattice size, we made 10^6 measurements after discarding 10^5 iterations for equilibration. For $L \leq 512$ we performed a single long run starting from the ordered state 0/1. For $L = 1024$ we made two independent runs with different initial conditions, one starting in the ordered state 0/1 and the other starting in the ideal state 0/12 (each individual run was of total length 6×10^5 , with the first 10^5 iterations discarded); there was no noticeable disagreement between the two sets of results. In units of the longest autocorrelation time $\tau_{\text{int}, \mathcal{P}_{\text{stagg}}^2}$ (see below), our run length corresponds to $\approx 1.3 \times 10^5 \tau_{\text{int}}$ measurements, and our discard interval corresponds to $\approx 1.3 \times 10^4 \tau_{\text{int}}$ iterations. This run length is sufficient to get a high-precision determination of both static and dynamic observables: we obtain errors of order $\lesssim 0.2\%$ for the static observables and of order $\lesssim 2\%$ for the dynamic ones.¹⁴

Our program was written in FORTRAN. The runs for $L \leq 512$ were carried out on a Pentium 166 machine: each WSK iteration took approximately $5.7 L^2 \mu\text{sec}$. The runs for $L = 1024$ were carried out on an IBM RS-6000/370 workstation, taking $8.5 L^2 \mu\text{sec}$ per iteration. The total CPU time used in this project was approximately 1 month on the former machine plus 4 months on the latter.

¹³ By contrast, the WSK algorithm for $q = 3$ is known to be *nonergodic* on periodic $3m \times 3n$ square lattices whenever m and n are relatively prime [32]. Other cases are open questions.

¹⁴ Our discard interval might seem to be much larger than necessary: $10^2 \tau_{\text{int}}$ would usually be more than enough. However, there is always the danger that the longest autocorrelation time in the system is much larger than the longest autocorrelation time that one has *measured*, because one has failed to measure an observable having sufficiently strong overlap with the slowest mode. (Here is a minor example of this effect: the authors of Refs. [6, 7] reported $\tau_{\text{int}} \lesssim 5$ because they failed to consider our slowest observable $\mathcal{P}_{\text{stagg}}$, which has autocorrelation time $\tau_{\text{int}, \mathcal{P}_{\text{stagg}}^2} \approx 8$.) As an undoubtedly overly conservative precaution against the possible (but unlikely) existence of such a (vastly) slower mode, we decided to discard approximately 10% of the entire run. This discard amounts to reducing the accuracy on our final estimates by a mere 5%.

Note also that while we have here performed our simulations only at zero temperature ($\beta = \infty$), the authors of Refs. [6, 7] employed a closely-spaced set of temperatures ranging from very high temperature ($\beta = 2.0$, $\xi \approx 5$) to very low temperature ($\beta = 6.0$, $\xi \approx 20000$) and found the autocorrelation times of $\mathcal{M}_{\text{stagg}}^2$ and the energy to be uniformly small. This constitutes further evidence against the existence of an undetected extremely slow mode.

The “zero-momentum” observables

$$\mathcal{M}_{stagg} = \sum_x \mathbf{M}_{stagg}(x) \quad (3.1)$$

$$\mathcal{M}_u = \sum_x \mathbf{M}_u(x) \quad (3.2)$$

$$\mathcal{P}_{stagg} = \sum_x \mathbf{P}_{stagg}(x) \quad (3.3)$$

all have mean zero. We have therefore measured their squares

$$\mathcal{M}_{stagg}^2 = \left(\sum_x \mathbf{M}_{stagg}(x) \right)^2 = \frac{3}{2} \sum_a \left| \sum_x (-1)^{x_1+x_2} \delta_{\sigma_x, a} \right|^2 \quad (3.4)$$

$$\mathcal{M}_u^2 = \left(\sum_x \mathbf{M}_u(x) \right)^2 = \frac{3}{2} \sum_a \left| \sum_x \delta_{\sigma_x, a} \right|^2 - \frac{V^2}{2} \quad (3.5)$$

$$\mathcal{P}_{stagg}^2 = \left(\sum_x \mathbf{P}_{stagg}(x) \right)^2 = \left| \sum_{\langle xy \rangle \text{ nnn}} (-1)^{x_1+x_2} \delta_{\sigma_x, \sigma_y} \right|^2 \quad (3.6)$$

as well as the “smallest-nonzero-momentum” observable associated to $\mathbf{M}_{stagg}(x)$:

$$\begin{aligned} \mathcal{F}_{stagg} &= \frac{1}{2} \left\{ \left| \sum_x e^{2\pi i x_1/L} \mathbf{M}_{stagg}(x) \right|^2 + \left| \sum_x e^{2\pi i x_2/L} \mathbf{M}_{stagg}(x) \right|^2 \right\} \\ &= \frac{3}{2} \times \frac{1}{2} \sum_a \left\{ \left| \sum_x (-1)^{x_1+x_2} e^{2\pi i x_1/L} \delta_{\sigma_x, a} \right|^2 + \left| \sum_x (-1)^{x_1+x_2} e^{2\pi i x_2/L} \delta_{\sigma_x, a} \right|^2 \right\}. \end{aligned} \quad (3.7)$$

Here $V = L^2$ is the volume of the system, the sum \sum_a is over the three possible values of the Potts spins, and the sum $\sum_{\langle xy \rangle \text{ nnn}}$ is over all pairs of diagonal-next-nearest neighbors x, y (each pair taken only once). The staggered and uniform susceptibilities are given by

$$\chi_{stagg} = \frac{1}{V} \langle \mathcal{M}_{stagg}^2 \rangle \quad (3.8)$$

$$\chi_u = \frac{1}{V} \langle \mathcal{M}_u^2 \rangle \quad (3.9)$$

and the “susceptibility” associated to the observable \mathcal{P}_{stagg} is

$$\chi_{\mathcal{P}_{stagg}} = \frac{1}{V} \langle \mathcal{P}_{stagg}^2 \rangle. \quad (3.10)$$

Finally, the second-moment correlation length is defined by

$$\xi = \frac{[(\chi_{stagg}/F_{stagg}) - 1]^{1/2}}{2 \sin(\pi/L)}, \quad (3.11)$$

where

$$F_{\text{stagg}} = \frac{1}{V} \langle \mathcal{F}_{\text{stagg}} \rangle . \quad (3.12)$$

The results of our simulations for the mean values of all these static observables are displayed in Table 2.

We have also measured the integrated autocorrelation time associated to each of the basic observables, using a self-consistent truncation window of width $6\tau_{\text{int}}$ [33, Appendix C]. We find that the largest autocorrelation time (of the observables we measured) corresponds to $\mathcal{P}_{\text{stagg}}^2$, though all of them are roughly of the same order of magnitude (Table 3). None of these autocorrelation times diverges as L grows; they tend to a constant. We have fitted the autocorrelation time for each observable to a constant (using methods to be described at the beginning of the next section). Our best fits are:

$$\tau_{\text{int}, \mathcal{P}_{\text{stagg}}^2} = 7.552 \pm 0.052 \quad (L_{\min} = 128, \chi^2 = 5.43, 3 \text{ DF}) \quad (3.13)$$

$$\tau_{\text{int}, \mathcal{M}_u^2} = 4.921 \pm 0.027 \quad (L_{\min} = 128, \chi^2 = 1.87, 3 \text{ DF}) \quad (3.14)$$

$$\tau_{\text{int}, \mathcal{M}_{\text{stagg}}^2} = 4.528 \pm 0.028 \quad (L_{\min} = 256, \chi^2 = 0.56, 2 \text{ DF}) \quad (3.15)$$

$$\tau_{\text{int}, \mathcal{F}_{\text{stagg}}} = 3.804 \pm 0.015 \quad (L_{\min} = 32, \chi^2 = 4.81, 5 \text{ DF}) \quad (3.16)$$

We conclude that the WSK algorithm for this model at $T = 0$ has no critical slowing-down [6, 7]: $\tau_{\text{int}} \lesssim 8$ uniformly in L .

4 Data Analysis

We perform all fits using the standard weighted least-squares method. As a precaution against corrections to scaling, we impose a lower cutoff $L \geq L_{\min}$ on the data points admitted in the fit, and we study systematically the effects of varying L_{\min} on both the estimated parameters and the χ^2 . In general, our preferred fit corresponds to the smallest L_{\min} for which the goodness of fit is reasonable (e.g., the confidence level¹⁵ is $\gtrsim 10\text{--}20\%$) and for which subsequent increases in L_{\min} do not cause the χ^2 to drop vastly more than one unit per degree of freedom.

4.1 Staggered Susceptibility

The theoretically expected behavior of the staggered susceptibility at criticality (i.e., at zero temperature) is

$$\chi_{\text{stagg}} = L^{(\gamma/\nu)_{\text{stagg}}} [A + BL^{-\Delta} + \dots] \quad (4.1)$$

¹⁵ “Confidence level” is the probability that χ^2 would exceed the observed value, assuming that the underlying statistical model is correct. An unusually low confidence level (e.g., less than 5%) thus suggests that the underlying statistical model is *incorrect* — the most likely cause of which would be corrections to scaling.

with $(\gamma/\nu)_{stagg} = 5/3$; here Δ is a correction-to-scaling exponent and the dots indicate higher-order corrections to scaling. Based on the numerical results of Refs. [6, 7], we do not expect large corrections to scaling on this observable.

We tried first to extract the leading term in (4.1) by fitting our data to a simple power-law Ansatz $\chi_{stagg} = AL^{(\gamma/\nu)_{stagg}}$. This fit is reasonable already for $L_{min} = 32$ ($\chi^2 = 4.34$, 4 DF, level = 36%), but our preferred fit is $L_{min} = 128$:

$$\left(\frac{\gamma}{\nu}\right)_{stagg} = 1.66621 \pm 0.00035 \quad (4.2)$$

with $\chi^2 = 1.31$ (2 DF, confidence level = 52%). This result is only 1.5 standard deviations away from the expected value 5/3.

We then considered the Ansatz (4.1), imposing the leading exponent $(\gamma/\nu)_{stagg} = 5/3$ and trying various values for the first correction-to-scaling exponent Δ . We are able to find reasonably good fits already for $L_{min} = 4$, provided we take Δ in the range $1.50 \lesssim \Delta \lesssim 1.76$. We therefore performed a three-parameter nonlinear weighted least-squares fit to simultaneously estimate A , B and Δ . Using $L_{min} = 4$, we obtain

$$\Delta = 1.624 \pm 0.061 \quad (4.3)$$

with $\chi^2 = 7.30$ (6 DF, level = 29%).

It is interesting to note that the exponent 5/3 is included in the interval (4.3). If this is the true behavior, it means that the leading correction to pure power-law behavior in the staggered susceptibility is merely an additive constant:

$$\chi_{stagg} = 0.87696(17)L^{5/3} - 0.2820(30) \quad (4.4)$$

with $\chi^2 = 7.78$ (7 DF, level = 35%). Such a correction can be interpreted as a mere lattice artifact, not necessarily arising from any irrelevant operator of the continuum theory.

4.2 Uniform Susceptibility

The theoretically expected behavior for the uniform susceptibility is

$$\chi_u = L^{(\gamma/\nu)_u} [A + BL^{-\Delta} + \dots] \quad (4.5)$$

with $(\gamma/\nu)_u = 2/3$. The simple power-law Ansatz gives a decent fit only for $L_{min} = 256$, yielding

$$\left(\frac{\gamma}{\nu}\right)_u = 0.6705 \pm 0.0022 \quad (4.6)$$

with $\chi^2 = 0.35$ (1 DF, level = 55%). This result is 1.75 standard deviations away from the theoretical prediction.

The large deviations from pure power-law behavior for $L < 256$ can be explained as an effect of corrections to scaling. Indeed, if we consider the Ansatz (4.5) with $(\gamma/\nu)_u = 2/3$ imposed and with just one correction-to-scaling term, we can obtain sensible fits even for $L_{min} = 4$. But in this case, in contrast to the preceding one,

the range of acceptable Δ values is much narrower: $0.655 \lesssim \Delta \lesssim 0.735$. A three-parameter nonlinear weighted least-squares fit to A , B and Δ , with $L_{min} = 4$, yields

$$\Delta = 0.695 \pm 0.013 \quad (4.7)$$

with $\chi^2 = 1.96$ (6 DF, level = 92%). In this case the value $\Delta = 2/3$ is two standard deviations away from the above estimate, but the absolute discrepancy is small (less than 0.03) and can plausibly be explained as an effect of higher-order corrections to scaling. Indeed, the uniform susceptibility can be fitted well (with $L_{min} = 4$) as a pure power law plus an additive constant:

$$\chi_u = 0.54744(49)L^{2/3} - 0.3486(16). \quad (4.8)$$

with $\chi^2 = 7.15$ (7 DF, level = 41%).

The results (4.3)/(4.4) and (4.7)/(4.8), taken together, suggest that there are no irrelevant operators (having the symmetries of the Hamiltonian) with $\Delta < 5/3$ and that the leading corrections to scaling in both χ_{stagg} and χ_u are lattice artifacts. This behavior is consistent with the prediction (2.15) that the leading irrelevant operator is $(\nabla \bar{h})^4$, with $\Delta = 2$.

4.3 Staggered Polarization

The finite-size-scaling behavior of $\chi_{P_{stagg}}$ is expected to be

$$\chi_{P_{stagg}} = \chi_{P_{stagg}}(\infty) + BL^{-\Delta} + \dots \quad (4.9)$$

with $\Delta = 1$. We tried first to ignore the correction-to-scaling term and fit the data to a constant. The fit is not very good: even for $L_{min} = 128$ we have $\chi^2 = 6.68$ (3 DF, level = 8%), with the estimate

$$\chi_{P_{stagg}}(\infty) = 2.1736 \pm 0.0060, \quad (4.10)$$

and the confidence level gets slightly worse for $L_{min} = 256, 512$.

We next fit to (4.9) with $\Delta = 1$. For $L_{min} = 8$ one already gets a fair (though not spectacular) fit:

$$\chi_{P_{stagg}}(\infty) = 2.1728 \pm 0.0054 \quad (4.11)$$

with $\chi^2 = 9.63$ (6 DF, level = 14%). However, the confidence level does not improve significantly for larger L_{min} .

We also tried fits to (4.9) with various values $\Delta \neq 1$. We were able to get reasonable fits for $L_{min} = 8$, if we take $0.50 \lesssim \Delta \lesssim 1.05$. We then tried a three-parameter fit to obtain estimates for $\chi_{P_{stagg}}(\infty)$, B and Δ . Our preferred fit corresponds to $L_{min} = 8$:

$$\chi_{P_{stagg}}(\infty) = 2.160 \pm 0.011 \quad (4.12a)$$

$$\Delta = 0.75 \pm 0.12 \quad (4.12b)$$

with $\chi^2 = 6.39$ (5 DF, level = 27%). The discrepancy between the above result and the predicted value $\Delta = 1$ is only two standard deviations; it might be due to higher-order corrections.

4.4 Correlation Length

Finally, we consider the scaling behavior of the second-moment correlation length, which is expected to be of the form

$$\xi = L^p [x^* + BL^{-\Delta} + \dots] \quad (4.13)$$

with $p = 1$.

First, we tried to estimate the power p by a simple power-law fit. This gives a good result for $L_{min} = 128$:

$$p = 0.99875 \pm 0.00069 \quad (4.14)$$

with $\chi^2 = 0.48$ (2 DF, level = 79%). This estimate is only 1.8 standard deviations away from the expected value $p = 1$, and the very small discrepancy (less than 0.0013) can be explained as an effect of corrections to scaling.

If we look at Table 4, we see that the ratio ξ/L increases from $L = 4$ to $L = 8$, decreases monotonically from $L = 8$ to $L = 64$, and then oscillates due to statistical noise for $L > 64$. Thus, if we want to study the $L \rightarrow \infty$ limit of this quantity *without* including correction-to-scaling terms, we expect to get a reasonable fit only for $L_{min} \geq 64$. Indeed, if we fit our data to a constant x^* , the first decent fit occurs for $L_{min} = 64$, giving

$$x^* = 0.63546 \pm 0.00030 \quad (4.15)$$

with $\chi^2 = 3.77$ (4 DF, level = 44%). However, our preferred fit corresponds to $L_{min} = 512$,

$$x^* = 0.63483 \pm 0.00048 \quad (4.16)$$

with $\chi^2 = 0.0051$ (1 DF, level = 94%).

On the other hand, if we want to study corrections to scaling, we must use at least some of the data with $L \leq 64$. The non-monotonic behavior for $4 \leq L \leq 64$ indicates that, to obtain a reasonable fit over this whole interval, we would need at least *two* correction-to-scaling terms with amplitudes of *opposite* sign. An Ansatz with only one correction-to-scaling term could, at best, fit the data with $L_{min} \geq 8$, and very likely not even that.

Indeed, if we fit the data to the Ansatz (4.13) with $p = 1$ and only one correction-to-scaling term $\sim L^{-\Delta}$, we find that reasonably good fits are obtained for $0.25 \lesssim \Delta \lesssim 0.60$ with $L_{min} = 8$. (For $L_{min} = 4$ we were unable to find any good fit, as expected.) We next tried a three-parameter fit to estimate x^* , B and Δ . The first reasonably good fit corresponds again to $L_{min} = 8$, and the estimates are

$$x^* = 0.63359 \pm 0.00132 \quad (4.17a)$$

$$\Delta = 0.42 \pm 0.16 \quad (4.17b)$$

with $\chi^2 = 9.35$ (5 DF, level = 10%). However, a better fit is obtained with $L_{min} = 16$, giving

$$x^* = 0.63479 \pm 0.00066 \quad (4.18a)$$

$$\Delta = 0.84 \pm 0.32 \quad (4.18b)$$

with $\chi^2 = 5.95$ (4 DF, level = 20%). For $L_{min} \geq 32$, we do not get any sensible result (Δ and B become very large, along with their error bars); this is due to the fact that most of these data correspond to the regime $L \geq 64$ where the corrections to scaling are submerged under the statistical noise. Let us remark that the value of x^* given in (4.18a) is only 1.6 standard deviations away from the one estimated by Ferreira and Sokal [7] using extrapolation techniques at nonzero temperature:

$$x_{FS}^* \approx 0.633888 . \quad (4.19)$$

If we want to fit *all* the data (i.e. take $L_{min} = 4$), we should introduce at least two correction-to-scaling terms. From the definition (3.11), we expect two types of corrections to scaling for the correlation length: one of order $L^{-5/3}$ coming from the numerator [cf. (4.4)], and another of order L^{-2} coming from the subleading terms in the sine. Furthermore, we might also expect an effective constant-term ‘‘correction’’ of order L^{-1} , analogously to what happened for the two susceptibilities. Thus, our next Ansatz would be

$$\frac{\xi}{L} = x^* + BL^{-1} + CL^{-5/3} . \quad (4.20)$$

If the coefficients B and C have different signs, the contribution of these two terms could be mimicked (in the range of monotonicity, $L_{min} \geq 8$) by a single correction term with an exponent $\Delta_{eff} < 1$, where Δ_{eff} increases towards 1 as $L_{min} \rightarrow \infty$. Indeed, this scenario is in good agreement with our results (4.17b)/(4.18b). We therefore tried a three-parameter fit directly to the Ansatz (4.20). Our preferred fit corresponds to $L_{min} = 4$:

$$x^* = 0.63457 \pm 0.00033 \quad (4.21a)$$

$$B = 0.182 \pm 0.014 \quad (4.21b)$$

$$C = -0.521 \pm 0.035 \quad (4.21c)$$

with $\chi^2 = 7.01$ (6 DF, level = 32%). This result certainly does not *prove* that the Ansatz (4.20) is correct, since many other pairs of correction-to-scaling exponents could give an equally good fit; but it does display a satisfying agreement.

Acknowledgments

We wish to thank Chris Henley for valuable correspondence and for making available some of his unpublished notes.

J.S. gratefully acknowledges the hospitality of the Department of Physics at New York University, where this work was finished. The authors’ research was supported in part by CICYT grants PB95-0797 and AEN97-1680 (J.S.) and by U.S. National Science Foundation grant PHY-9520978 (A.D.S. and J.S.).

References

- [1] R.B. Potts, Proc. Camb. Philos. Soc. **48**, 106 (1952).
- [2] F.Y. Wu, Rev. Mod. Phys. **54**, 235 (1982); **55**, 315 (E) (1983).
- [3] F.Y. Wu, J. Appl. Phys. **55**, 2421 (1984).
- [4] R. Kotecký, cited in H.-O. Georgii, *Gibbs Measures and Phase Transitions* (de Gruyter, Berlin–New York, 1988), pp. 148–149, 457.
- [5] J. Salas and A.D. Sokal, J. Stat. Phys. **86**, 551 (1997).
- [6] S.J. Ferreira and A.D. Sokal, Phys. Rev. B**51**, 6727 (1995).
- [7] S.J. Ferreira and A.D. Sokal, in preparation.
- [8] R. Shrock and S.–H. Tsai, J. Phys. A **34**, 495 (1995).
- [9] J. Salas, in preparation.
- [10] M. den Nijs, M.P. Nightingale and M. Schick, Phys. Rev. B **26**, 2490 (1982).
- [11] H.W.J. Blöte and H.J. Hilhorst, J. Phys. A **15**, L631 (1982).
- [12] B. Nienhuis, H.J. Hilhorst and H.W.J. Blöte, J. Phys. A **17**, 3559 (1984).
- [13] J. Kolafa, J. Phys. A **17**, L777 (1984).
- [14] L.S. Levitov, Phys. Rev. Lett. **64**, 92 (1990).
- [15] W.P. Thurston, Amer. Math. Monthly **97**, 757 (1990).
- [16] D.A. Huse and A.D. Rutenberg, Phys. Rev. B **45**, 7536 (1992).
- [17] H.W.J. Blöte and B. Nienhuis, Phys. Rev. Lett. **72**, 1372 (1994).
- [18] J. Kondev and C.L. Henley, Phys. Rev. Lett. **73**, 2786 (1994).
- [19] J. Kondev and C.L. Henley, Phys. Rev. B **52**, 6628 (1995).
- [20] J. Kondev and C.L. Henley, Nucl. Phys. B **464**, 540 (1996).
- [21] J. Kondev, J. de Gier and B. Nienhuis, J. Phys. A **29**, 6489 (1996).
- [22] J. Kondev, Loop models, marginally rough interfaces, and the Coulomb gas, [cond-mat/9607181](#), to appear in the proceedings of the symposium on “Exactly Soluble Models in Statistical Mechanics” (March 1996, Northeastern University, Boston).
- [23] R. Raghavan, C.L. Henley and S.L. Arouh, J. Stat. Phys. **86**, 517 (1997).

- [24] C. Zeng and C.L. Henley, Phys. Rev. B **55**, 14935 (1997).
- [25] C.L. Henley, J. Stat. Phys. **89**, 483 (1997).
- [26] J.K. Burton Jr. and C.L. Henley, A constrained Potts antiferromagnet model with an interface representation, [cond-mat/9708171](#), submitted to J. Phys. A.
- [27] C.L. Henley, private communications.
- [28] P. Ginsparg, in *Fields, Strings and Critical Phenomena*, edited by E. Brézin and J. Zinn-Justin (North Holland, Amsterdam 1989).
- [29] H. Park and M. Widom, Phys. Rev. Lett. **63**, 1193 (1989).
- [30] J.-S. Wang, R.H. Swendsen and R. Kotecký, Phys. Rev. Lett. **63**, 109 (1989).
- [31] J.-S. Wang, R.H. Swendsen and R. Kotecký, Phys. Rev. B **42**, 2465 (1990).
- [32] M. Lubin and A.D. Sokal, Phys. Rev. Lett. **71**, 1778 (1993).
- [33] N. Madras and A.D. Sokal, J. Stat. Phys. **50**, 679 (1988).

Operator	G	η	$\gamma/\nu = 2 - \eta$	Numerical Result
\mathbf{M}_{stagg}	$\pm\pi/3$	1/3	5/3	1.66621 ± 0.00035
\mathbf{M}_u	$\pm 2\pi/3$	4/3	2/3	0.6705 ± 0.0022
\mathbf{P}_{stagg}	$\pm\pi$	3	-1	-0.75 ± 0.12

Table 1: Critical operators for the 3-state antiferromagnetic Potts model on the square lattice at zero temperature. The last column indicates the results from our Monte Carlo simulation (Section 4).

L	χ_{stagg}	χ_u	$\chi_{P_{stagg}}$	ξ
4	8.5576 ± 0.0024	1.0443 ± 0.0010	2.4486 ± 0.0076	2.5127 ± 0.0023
8	27.7671 ± 0.0120	1.8614 ± 0.0028	2.3888 ± 0.0124	5.1306 ± 0.0055
16	88.8206 ± 0.0441	3.1537 ± 0.0058	2.2882 ± 0.0128	10.2497 ± 0.0110
32	282.8085 ± 0.1477	5.2052 ± 0.0105	2.2464 ± 0.0126	20.4422 ± 0.0219
64	897.3520 ± 0.4776	8.4362 ± 0.0179	2.2110 ± 0.0124	40.6662 ± 0.0433
128	2851.2642 ± 1.5484	13.5899 ± 0.0296	2.1826 ± 0.0120	81.4388 ± 0.0880
256	9056.7475 ± 4.8888	21.8141 ± 0.0479	2.1852 ± 0.0122	162.8235 ± 0.1745
512	28731.6260 ± 15.5273	34.7753 ± 0.0767	2.1480 ± 0.0116	325.0478 ± 0.3449
1024	91167.3235 ± 49.2042	55.2604 ± 0.1240	2.1806 ± 0.0120	650.0264 ± 0.6924

Table 2: Mean values of the static observables for the 3-state square-lattice Potts antiferromagnet at zero temperature.

L	$\tau_{\text{int}, \mathcal{M}_{\text{stagg}}^2}$	$\tau_{\text{int}, \mathcal{M}_u^2}$	$\tau_{\text{int}, \mathcal{P}_{\text{stagg}}^2}$	$\tau_{\text{int}, \mathcal{F}_{\text{stagg}}}$
4	2.487 ± 0.020	1.525 ± 0.010	5.038 ± 0.057	3.330 ± 0.030
8	4.073 ± 0.041	3.240 ± 0.029	7.456 ± 0.101	4.032 ± 0.041
16	4.417 ± 0.046	4.154 ± 0.042	7.845 ± 0.109	3.850 ± 0.038
32	4.488 ± 0.047	4.628 ± 0.049	7.765 ± 0.107	3.826 ± 0.037
64	4.483 ± 0.047	4.803 ± 0.052	7.863 ± 0.110	3.803 ± 0.037
128	4.587 ± 0.049	4.903 ± 0.054	7.528 ± 0.103	3.855 ± 0.038
256	4.558 ± 0.049	4.908 ± 0.054	7.686 ± 0.106	3.816 ± 0.037
512	4.515 ± 0.048	4.889 ± 0.054	7.377 ± 0.100	3.752 ± 0.036
1024	4.512 ± 0.048	4.986 ± 0.056	7.638 ± 0.105	3.776 ± 0.037

Table 3: Mean values of the dynamic observables for the 3-state square-lattice Potts antiferromagnet at zero temperature.

L	ξ/L
4	0.62818 ± 0.00057
8	0.64133 ± 0.00069
16	0.64061 ± 0.00069
32	0.63882 ± 0.00068
64	0.63541 ± 0.00068
128	0.63624 ± 0.00069
256	0.63603 ± 0.00068
512	0.63486 ± 0.00067
1024	0.63479 ± 0.00068

Table 4: Values of the ratio ξ/L for the 3-state square-lattice Potts antiferromagnet at zero temperature.

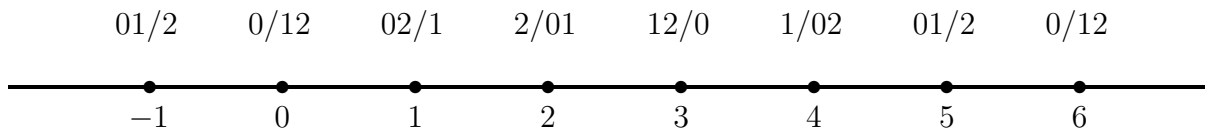


Figure 1: Ideal-state lattice \mathcal{I} for the 3-state square-lattice Potts antiferromagnet. The symbols above the graph indicate the ideal states of the spin model: 0/12 means that the spins on the even sublattice are all equal to 0 and that the spins on the odd sublattice are chosen randomly between the values 1 and 2. The numbers below the graph indicate the average height for the given ideal state; this height is determined modulo 6.

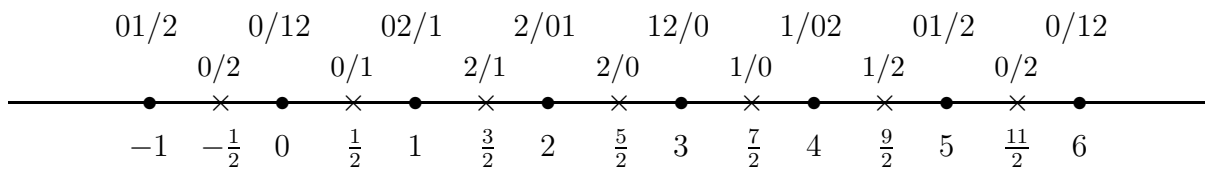


Figure 2: The average height $\tilde{h}(x)$ on a plaquette is uniquely determined modulo 6 by the spin content of that plaquette: 0/12 means, for example, that the two spins belonging to the even sublattice are both equal to 0, while the two spins belonging to the odd sublattice are 1 and 2.